

Review

# A Critical Review on the Performance of Pile-Supported Rail Embankments under Cyclic Loading: Numerical Modeling Approach

A. S. M. Riyad <sup>1,2</sup>, Fernanda Bessa Ferreira <sup>3,\*</sup>, Buddhima Indraratna <sup>1</sup> and Trung Ngo <sup>1</sup>

<sup>1</sup> Transport Research Centre, School of Civil and Environmental Engineering, University of Technology Sydney (UTS), Sydney, NSW 2007, Australia; A.S.Riyad@student.uts.edu.au (A.S.M.R.); Buddhima.Indraratna@uts.edu.au (B.I.); Trung.Ngo@uts.edu.au (T.N.)

<sup>2</sup> Department of Civil Engineering, Khulna University of Engineering & Technology, Khulna 9203, Bangladesh

<sup>3</sup> CONSTRUCT-Geo, Faculty of Engineering, University of Porto, 4200-465 Porto, Portugal

\* Correspondence: fbf@fe.up.pt

**Abstract:** Searching for economical and practical solutions to increase any transport substructure's protection and stability is critical for ensuring the long-term viability and adequate load-bearing capacity. Piles are increasingly being used as an economical and environmentally sustainable solution to enhance the strength of soft subgrade soils on which embankments are raised. As per the available literature, there are two main strategies used to explain railway embankments' performance: experimental approaches and numerical simulations on a broad scale. The purpose of this study is to examine the state-of-the-art literature on numerical modeling methods adopted to assess the performance of pile-supported rail embankments subjected to cyclic loading. The paper addresses the main results from various numerical methods to explain the appropriate mechanisms associated with the load deformation response. It also presents the key issues and drawbacks of these numerical methods concerning rail embankment development while outlining the specific shortcomings and research gaps relevant to enhanced future design and analysis.

**Keywords:** piled railway embankment; rail track substructure; cyclic loading; geosynthetic reinforcement; numerical simulation; FEM–DEM coupling



**Citation:** Riyad, A.S.M.; Ferreira, F.B.; Indraratna, B.; Ngo, T. A Critical Review on the Performance of Pile-Supported Rail Embankments under Cyclic Loading: Numerical Modeling Approach. *Sustainability* **2021**, *13*, 2509. <https://doi.org/10.3390/su13052509>

Academic Editor:  
Sakdirat Kaewunruen

Received: 1 February 2021  
Accepted: 18 February 2021  
Published: 26 February 2021

**Publisher's Note:** MDPI stays neutral with regard to jurisdictional claims in published maps and institutional affiliations.



**Copyright:** © 2021 by the authors. Licensee MDPI, Basel, Switzerland. This article is an open access article distributed under the terms and conditions of the Creative Commons Attribution (CC BY) license (<https://creativecommons.org/licenses/by/4.0/>).

## 1. Introduction

Railways across the globe are experiencing a revival in all areas, including metropolitan rail, high-speed rail, heavy haul, and intermodal freight operations. Owing to the usage of faster and heavier trains, conventional rail bases, or track substructures composed of one or more granular stratum overlying the soil subgrade have become rapidly weighed down. Railways constructed on terrains with adverse geotechnical conditions coupled with sub-standard substructures need routine maintenance to reach higher construction standards. Seeking economic and realistic strategies to improve the substructure's stability is crucial for ensuring the rail industry's long-term sustainability and providing an adequate capacity to sustain future load increases.

Much attention has been paid in the past to the above-ground track elements such as rails, rail pads, sleepers or ties, and fasteners [1]. However, numerous studies [2,3] have indicated that the majority of expenditure on track maintenance is normally spent on track substructure. The economic analyses of Wheat and Smith [4] based on UK rail systems found that more than one-third of the overall capital cost on all ballasted rail networks corresponds to the track substructure. As a consequence of severe ballast deterioration, the Australian rail sector invests a massive amount on regular track rehabilitation (e.g., over AUD 12 million per annum in the state of New South Wales alone), and substantial land development before track construction, where poor and deteriorated base soils (subgrade)

provide significant challenges [5]. For this reason, numerous research studies have been conducted to address the challenges of increasing demand for higher performance track substructure, and thereby to effectively manage the growing need for high-speed commuter lines as well as higher axle heavy haul railways [6,7].

The track substructure is considered as typically integrated with the geotechnical properties of a layered system comprising ballast, sub-ballast (including a capping layer), and structural fill (if required to raise an embankment) over the natural subgrade [8]. On the one hand, Indraratna and co-workers (e.g., [6,9–22]) gave special attention to selected components of track substructure, namely, ballast and sub-ballast. On the other hand, the behavior of railway subgrade or the rail embankment itself has gained less attention, albeit with their significant influence on the overall maintenance costs [23].

Since railway routes over troublesome subgrades—comprising poor, porous, expansive, as well as collapsible soils posing the threat of excessive or unacceptable deformation (e.g., [24])—are unavoidable in most real-life situations, efficient methods of soil improvement are necessary to ensure stability (e.g., [25]). A railroad embankment is constantly subjected to a significant range of axle loads and frequencies (speed) over its operational period. With the increase in repeated loads throughout the service life, the associated permanent deformation is inevitable, and the incremental accumulation of plastic strains over time may lead to unacceptable differential settlement and even the subgrade failure of the track.

The performance of unbound granular materials depends not only on their current physical properties but also on their changes that govern the long-term response under cyclic loading. The performance of these materials is often complicated due to the occurrence of both permanent as well as resilient strains and the degradation of particles under cyclic loading. The resilient response is vital to the load-bearing capacity of the embankment system, whereas the permanent strain response exemplifies the long-term efficiency of the embankment. One effect of such a granular composition is that unbound materials have no intrinsic strength as a continuum when untreated and are unable to sustain any tension. On the other hand, they can sustain (small) shear stresses [26]. For this reason, properly understanding the plastic behavior of unbound granular materials and the adoption of a correct constitutive model for numerical analysis are imperative.

Several researchers have examined the behavior of transport embankments under static loading [27–29]. However, railway embankments experience a cyclic response caused by moving axle loads. Various studies (e.g., [30–34]) have pointed out the influence of cyclic loads on soft soil (subgrade) compressibility and strength characteristics.

Pile-supported embankments have been widely used as a rapid construction method to reduce differential and total settlements and to enhance the load transfer mechanism from the soil to the piles over poor subgrade soil conditions [35,36]. This method has several benefits, including enhanced overall stability (bearing capacity), limited lateral and vertical deformations, and easy-to-control settlements from a design point of view [37,38]. Britton and Naughton [39] pointed out the benefits of this piled embankment approach over other techniques including geosynthetic soil reinforcement, stage construction, or preloading, using lightweight fill, over-excavation, and replacement. According to them, superstructures can be constructed in a single stage, avoiding extended construction periods while achieving a substantial reduction in both differential and total settlements.

The use of granular pile-supported embankments (such as stone columns and gravel piles) has increased nowadays compared to the traditional continuous concrete piles. Each method has its own advantages and disadvantages. Concrete piles cannot dissipate excess pore water pressure [40], while granular piles supporting embankments on soft soils can rapidly dissipate excess pore pressures while transferring load. Furthermore, granular piles can easily be made continuous and uniform with the base layer of an embankment, which can be a compacted granular layer consisting of the same granular medium as used for the piles; hence, this saves much time during construction. Granular piles supporting embankment can be composed of waste materials from industry such as coal wash, blast

furnace slag, mines waste rock, and discarded rail ballast, and hence are more economical than using concrete piles. Moreover, concrete piles do not serve the expectation of a favorable carbon footprint, while granular piles constructed using waste granulates uphold significant environmental benefits, including waste recycling and reducing quarrying of natural aggregates. In particular, granular piles can be constructed with marginal rockfills mixed with recycled rubber crumbs to act as energy-absorbing supports [41] for the overlying embankment, reducing vibrations and minimizing damage caused by impact forces to the infrastructure components. For example, railway ballast and concrete sleepers' damage due to heavy haul loading can be lessened by introducing granular pile-supported embankments. However, bulging and lateral movement of granular piles may occur under heavy loads [42–44], and hence the diameters need to be much larger than those of concrete piles if the applied live load is very high. The shear strength of granular piles supporting embankment will be less than that of typical concrete piles [45]. In addition, concrete piles are often quicker to install in the ground with well-established contractors and continuous piling methods. Finally, where waste granular aggregates or marginal rockfill is not locally available, granular piles may not be an attractive option compared to concrete that is readily available anywhere.

In a piled embankment, the embankment fill tends to settle more in the regions between piles because of stiffness variation between the piles and the surrounding soil. However, this downward displacement is restricted owing to shearing mechanisms in the fill. Due to mobilized shear resistance, the load is partially transferred onto the piles while the stress imposed on the soft ground is reduced. This load transfer mechanism is known as soil arching (Figure 1), as initially described by Terzaghi [46]. In a piled rail embankment (Figure 2), the soil arching phenomenon plays a key role in the efficient load transfer from the embankment to the piles [47]. Basal geosynthetic reinforcement is also often used, as it contributes to the load transfer onto the piles by the membrane effect (Figure 3). The proportion of load transferred onto the piles is usually referred to as efficacy.

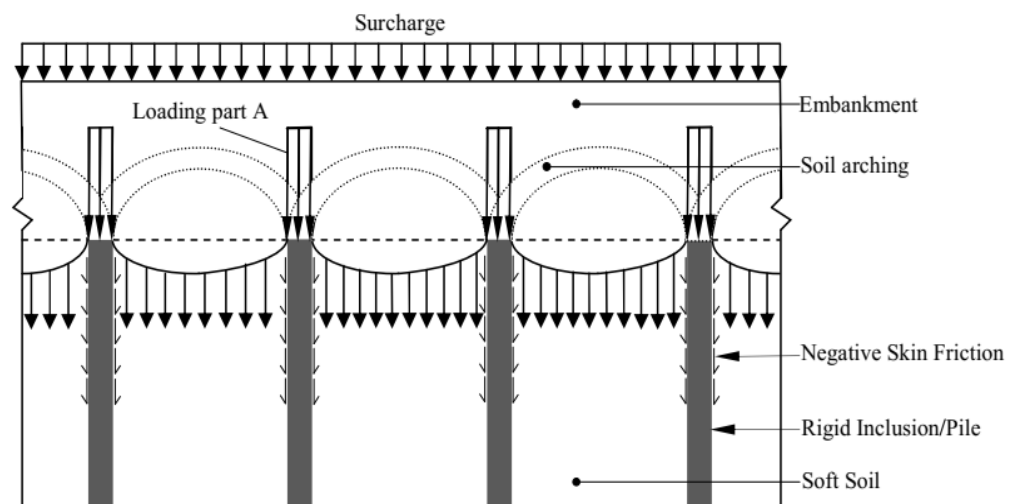


**Figure 1.** Schematic illustration of the load transfer mechanism of a pile-supported embankment (modified after [48]).

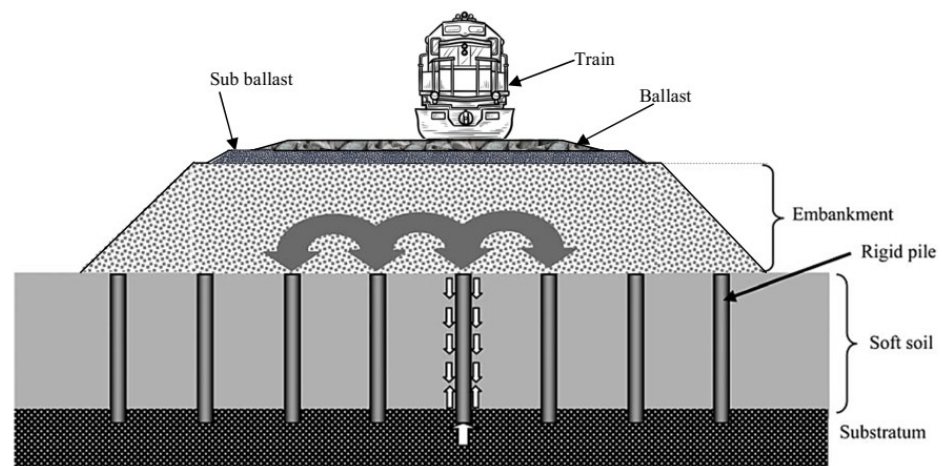


**Figure 2.** Schematic illustration of a piled railway embankment (republished with permission of American Society of Civil Engineers (ASCE), from [49]; permission conveyed through Copyright Clearance Center, Inc., Denver, MA, USA).

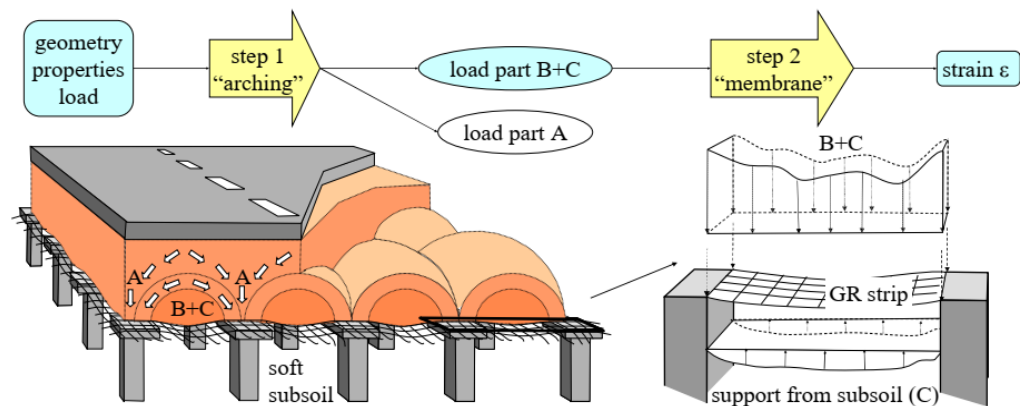


**Figure 3.** Load transfer mechanism and membrane effect on the basal reinforced piled embankment (republished with permission of ASCE, from [50]; permission conveyed through Copyright Clearance Center, Inc.).

To study piled embankments' behavior, numerous researchers have developed different model tests (e.g., [27,51–53]). These model experiments have primarily focused on the arching behavior of the embankment soil. In reality, the load distribution processes are far more complex than simply soil arching, as shown by various pilot-scale or full-scale studies (e.g., [54–59]).

Alternatively, the use of modeling approaches is increased over the years to explain the material performance, especially as computational resources are improved. Modeling methods build the expertise and resources required for predictions and offer essential supporting evidence when explaining material performance through empirical approaches. In addition to the proper understanding and knowledge of the material behavior under varying circumstances, these techniques can allow substantial financial savings within the design limits.

Although some scholars have proposed mathematical formulations that are compatible with their findings [37,60–62], there is a need for considerable effort to develop more general models and procedures that are both theoretically sound as well as widely applicable. Meanwhile, with the growing availability of computing resources, general-purpose theoretical methods have progressively been substituted by numerical techniques, of which the finite element approach is one of the most commonly used. The move from simplistic analytical models brought about changes in precision by substituting them with

sophisticated numerical simulations capable of evaluating particular corner cases involving complicated geometries, paving the way for the implementation of more accurate constitutive models as well as boundary conditions [63].

While most of the studies in the past were mainly focused on static loadings as per the authors' knowledge, this paper aims to provide a critical review of the existing literature to investigate the fundamental principles of the underlying mechanisms and influence of piles beneath rail embankments under cyclic loading through numerical modeling.

## 2. Numerical Simulation of Piled Embankments

Numerical simulation or computational modeling of pile-supported rail embankments principally refers to the methods used to solve a series of algebraic or differential equations or theoretical models numerically to explain such structures' performance under dynamic loading. Computational modeling requires choosing an acceptable series of equations to approximate the embankment system's actions under analysis and then solving equations through suitable numerical procedures as well as verification, validation, and calibration. There are two major computational approaches to model pile-supported embankments. They are the continuum approach and discrete element modeling (e.g., [64–66]).

### 2.1. Effects of Embankment Height and Material Properties

Numerous researchers have conducted multiple computational simulations [28,49,67–71] to examine the load transfer process in a pile-supported embankment. The numerical investigation by Han and Gabr [69] assessed the effect of embankment height, pile elastic modulus, and geosynthetics tensile stiffness on the process of load transfer. The degree of soil arching was evaluated in terms of the soil arching ratio,  $\rho$  (where  $\rho = 0$  represents complete soil arching and  $\rho = 1$  represents no soil arching). The authors observed that the soil arching ratio decreases with increasing the embankment fill height, increasing the pile material's elastic modulus and decreasing the geosynthetic reinforcement's tensile stiffness. Jenck et al. [28] detected that a shearing mechanism effectively controls the transfer of load onto the piles due to soil arching. Soil arching limits the embankment subsoil settlement by the load transfer mechanism onto the piles [47]. Jenck et al. [49] demonstrated an efficacy improvement with the increase of embankment height.

Several design methods use the critical height concept to estimate the magnitude of arching (Table 1). The critical height is the height from the pile's cap top to the plane of equal settlement in the embankment fill [72]. The concept of the plane of equal settlement was originally proposed by Marston [73], as illustrated in Figure 4. According to Naughton [72], the arching phenomenon is not predominant if the embankment height is less than the plane of equal settlement, and geosynthetic reinforcement will carry the applied traffic loads. However, when the embankment height exceeds the plane of equal settlement, geosynthetics will only carry the embankment filling load in the yielding zone, and the residual embankment and traffic loads will be transferred to the pile caps by the process of arching.

**Table 1.** Summary of design methods to determine the critical height.

Design Approach	Critical Height
Terzaghi [74]	2.5 ( $s-a$ )
Carsslon [75]	1.87 ( $s-a$ )
Hewlett and Randolph [52]	1.4 ( $s-a$ )
BS 8006 [76]	1.4 ( $s-a$ )
Horgan and Sarby [77]	1.545 ( $s-a$ ) to 1.92 ( $s-a$ )
Russell et al. [78]	$H$ (for ultimate limit state design)
van Eekelen et al. [79]	1.87 ( $s-a$ )
Kempfert et al. [80]	$s/2$
Naughton [72]	$((s-a)/2) e^{\pi/2 \tan \phi}$

Where  $s$ : spacing between the piles;  $a$ : size of the pile cap;  $H$ : embankment height;  $\phi$ : friction angle of the embankment fill.

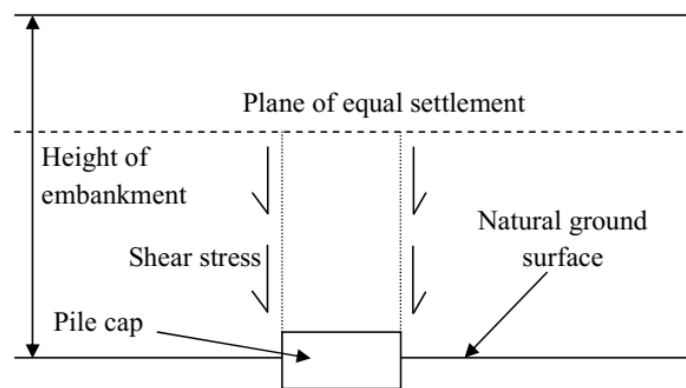


**Figure 4.** Plane of equal settlement (republished with permission of ASCE, from [72]; permission conveyed through Copyright Clearance Center, Inc.).

Low et al. [53] introduced a parameter, the stress reduction ratio ( $S_R$ ), which is the proportion of the mean vertical stress carried by the reinforcement and the average vertical stress induced by the embankment fill. Ariyaratne and Liyanapathirana [81] summarized various updated design approaches for geosynthetic-reinforced, pile-supported embankments (GRPS) considering  $S_R$  outlined in Table 2. Nevertheless, the arch shape is inconsistent in these design methods and different approximations and assumptions were used to derive the desired design equations. Consequently, several parameters (friction angle of the embankment fill, elastic modulus of the pile, and support to the foundation soil) were not considered in these design approaches, which establish the necessity of the adoption of numerical modeling approaches to incorporate all parameters [81].

**Table 2.** Design equations to determine the stress reduction ratio,  $S_R$  (adapted from [81]).

Basic Design Approach	Derived Design Equation
Terzaghi [46]	$S_R = \frac{(s^2 - a^2)}{4HaK \tan \phi} \left( 1 - e^{\frac{(-4HaK \tan \phi)}{(s^2 - a^2)}} \right)$ <p>where, <math>K = (1 - \sin \phi)</math></p>
Guido et al. [82]	$S_R = \frac{(s-a)}{3\sqrt{2}H}$
Hewlett and Randolph [52]	<p>Conditions at the crown</p> $S_R = \left(1 - \frac{a}{s}\right)^{2(K_P-1)} \left(1 - \frac{s \times 2(K_P-1)}{\sqrt{2}H(2K_P-3)} + \frac{(s-a) \times 2(K_P-1)}{\sqrt{2}H(2K_P-3)}\right)$ <p>Conditions at the pile cap</p> $S_R = \frac{1}{\left(\frac{2K_P}{(K_P+1)}\right) \left[ \left(1 - \frac{a}{s}\right)^{(1-K_P)} - \left(1 - \frac{a}{s}\right) \left(1 + \frac{a}{s} K_P\right) \right] + \left(1 - \frac{a^2}{s^2}\right)}$ <p>where, <math>K_P = \frac{(1 + \sin \phi)}{(1 - \sin \phi)}</math></p> <p>Maximum of these two values should be used in the design</p>
Low et al. [53]	$S_R = \frac{(\sigma_s - (tE_s/D))}{\gamma H}$
Kempfert et al. [80]	$S_R = \frac{1}{\gamma H} \left\{ \lambda_1^x \left( \gamma + \frac{q}{H} \right) \left[ H \left( \lambda_1 + h_g^2 \lambda_2 \right)^{-x} + h_g \left( \left( \lambda_1 + \frac{h_g^2 \lambda_2}{4} \right)^{-x} - \left( \lambda_1 + h_g^2 \lambda_2 \right)^{-x} \right) \right] \right\}$ <p>where,</p> $\lambda_1 = \frac{1}{8}(s_d - d)^2; \lambda_2 = \frac{s_d^2 + 2ds_d - d^2}{2s_d^2}; h_g = \frac{s_d}{2} \text{ for } H \geq \frac{s_d}{2}; h_g = H \text{ for } H < \frac{s_d}{2}$
BS 8006 [83]	<p>For partial arching,</p> $S_R = \frac{1}{(s^2 - a^2)} \left[ s^2 - a^2 \left( \frac{P_C}{\gamma H} \right) \right]$ <p>For full arching,</p> $S_R = \frac{1.4}{H(s+a)} \left[ s^2 - a^2 \left( \frac{P_C}{\gamma H} \right) \right]$

Where  $s$ : spacing between piles;  $a$ : size of pile cap;  $H$ : embankment height;  $K_p$ : earth pressure coefficient at rest;  $K_P$ : passive earth pressure coefficient;  $\phi$ : friction angle of embankment fill;  $\sigma_s$ : vertical stress on the foundation soil midway between piles;  $t$ : maximum vertical displacement of the foundation soil midway between pile caps;  $E_s$ : elastic modulus of foundation soil;  $D$ : depth of foundation soil;  $\dot{\lambda}$ : unit weight of embankment fill;  $d$ : pile diameter;  $h_g$ : arching height;  $q$ : surcharge;  $s_d$ : diagonal pile spacing;  $P_C$ : vertical stress on the pile.

Ariyaratne et al. [67] investigated the performance of pile-supported embankment in two-dimensional (2D) as well as three-dimensional (3D) conditions. They used different methods of idealization in 2D plain-strain conditions. Among them, the equivalent area (EA) method provided the closest outcomes to field test results and 3D numerical analysis.

Bhasi and Rajagopal [68] investigated the effect of embankment fill properties, pile modulus, and geosynthetic stiffness on the time-dependent behavior of piled embankments using 2D and 3D models. The authors found out that the friction angle of the embankment fills influences efficacy. To investigate soil arching's mechanical behavior, Li et al. [70] simulated the interaction among the pile, embankment fill, and subsoil in their numerical finite element model (FEM). They concluded that soil arching occurs after differential settlement since the equal settlement plane's height is not consistent with that of the critical arch. Their study also showed that soil arching's maximum intensity could be determined by defining the pile spacing.

## 2.2. Effects of Cyclic Loading Condition

### 2.2.1. Use of Continuum Approach

Pham and Dias [71] studied the performance of pile-supported embankments under different cyclic loading conditions considering the 3D numerical approach. They reported that constitutive models directly influence piled embankments' performance subjected to cyclic loading in terms of cumulative settlements and soil arching mechanism. The embankment and soft soil's cumulative settlements were particularly significant during the initial 300 load cycles, whereas the displacement of the pile head was almost negligible during all cyclic loading (Figure 5). A slight increase in the arching ratio was observed after 1000 load cycles for the traffic speed (V) of 100 km/h (Figure 6). The authors also studied the influence of traffic speed on the cumulative settlements, as shown in Figure 7. The traffic speed was found to have a relevant influence on the permanent settlements at the embankment crest (Figure 7a). Moreover, the higher the vehicle speed, the faster the permanent settlement of the soft soil (Figure 7b).

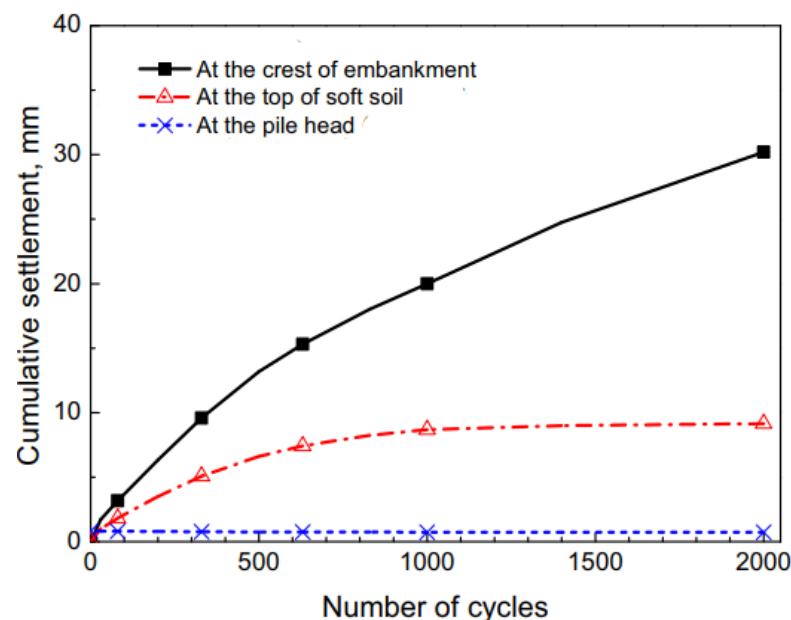


**Figure 5.** Effect of the number of load cycles on the cumulative settlement (republished with permission of ASCE, from [71]; permission conveyed through Copyright Clearance Center, Inc.).

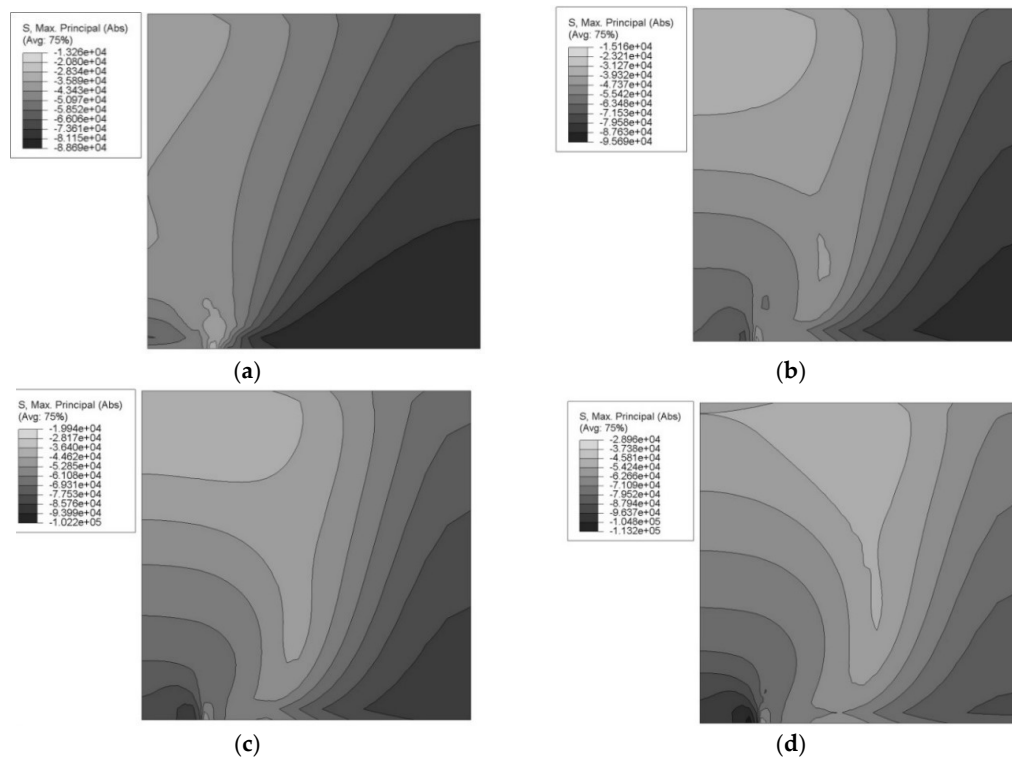


**Figure 6.** Schematic visualization of arching effect within the embankment fill (unit cell) with  $V = 100$  km/h: (a) after 300 cycles, (b) after 1000 cycles, (c) after 1400 cycles, and (d) after 2000 cycles (republished with permission of ASCE, from [71]; permission conveyed through Copyright Clearance Center, Inc.).

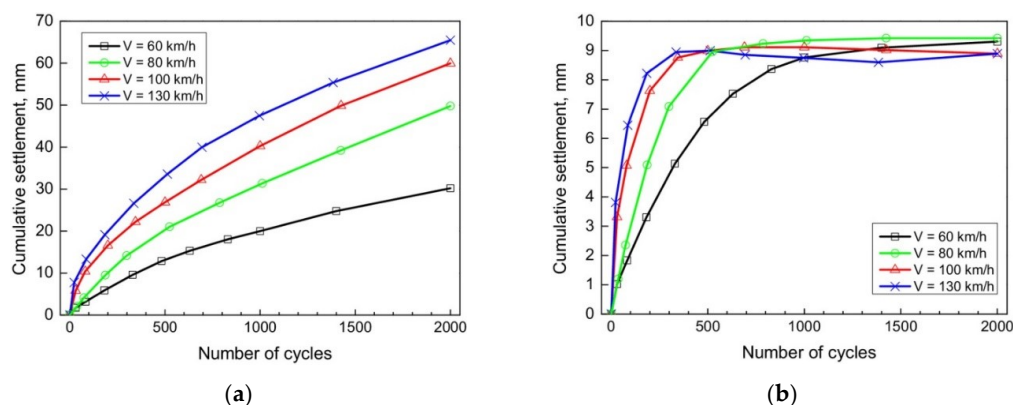


**Figure 7.** Effect of traffic speed on the permanent settlements: (a) embankment crest, (b) soft soil (republished with permission of ASCE, from [71]; permission conveyed through Copyright Clearance Center, Inc.).

Nunez et al. [84] compared the monitoring data of an experimental full-scale piled embankment with several analytical and 3D numerical design approaches and reported that the considered design approaches overestimated the stress reduction ratio or stress efficacy. Conversely, the settlement efficacy (based on the ratio of settlement with and without piles) was an important parameter to determine the pile-supported embankment's overall performance.

Meena et al. [47] investigated the performance of piled rail embankments using 2D plane strain conditions. The authors addressed the impact of train-induced loading and piles' arrangement on the stability of the railway embankment. The authors found that the settlement ratio ( $\delta_{em}/\delta_p$ ) decreased with the increase in train speed (Figure 8a). Moreover, for smaller pile spacing, the soil arching ratio (SAR) decreased with increasing train speed, whereas for larger pile spacing, the influence of train speed on SAR ( $\sigma_s/\gamma h+q$ ) was

negligible (Figure 8b). They also reported that the triangularly arranged piles demonstrated a more effective load transfer mechanism than the traditional square pattern (Figure 9). According to them, embankment height, pile and embankment modulus, pile spacing, and friction angle significantly affect the pile-supported railway embankment behavior. They also observed that plain strain numerical simulations provide inconsistent outcomes with the existing design approaches as the piled rail embankment consists of a 3D problem.

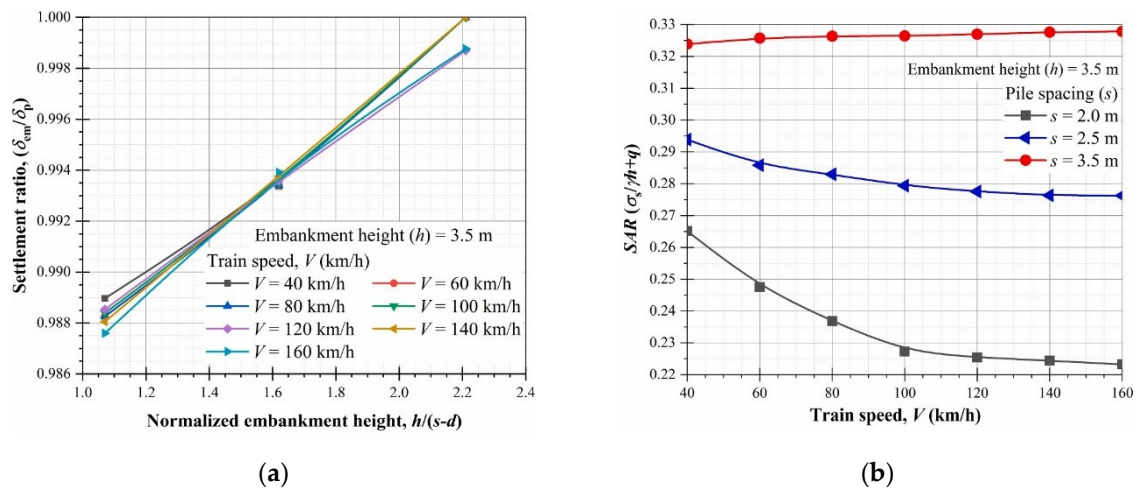


**Figure 8.** Influence of train speed on (a) settlement ratio, (b) soil arching ratio (SAR) (reprinted from [47], with permission from Elsevier, Amsterdam, The Netherlands).

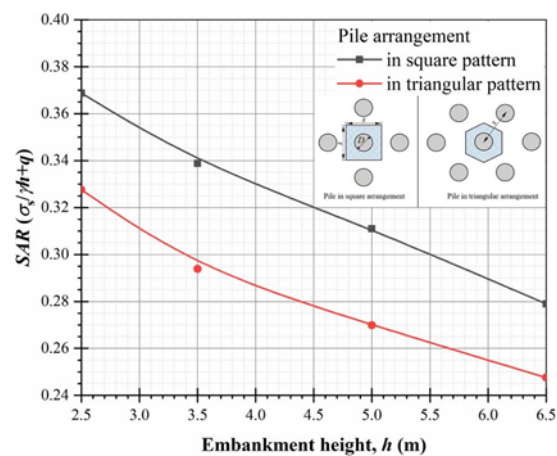


**Figure 9.** Effect of pile arrangement (reprinted from [47], with permission from Elsevier).

Pham et al. [85] used advanced FEM software (ABAQUS) to study geosynthetic-reinforced piled embankment behavior subjected to cyclic loading by 3D numerical modeling. Their research used the hypo-plasticity concept for the embankment fill and the modified cam-clay constitutive model for the soft soil to simulate the complex behavior during load cycles. They reported that the hypoplastic constitutive model provides better results concerning the embankment fills subjected to cyclic loading. They also stated that geosynthetics' presence reduced the cumulative settlements and slowed down the decrease in arching of the soil. However, the amount of geosynthetic layers did not show any significant improvement concerning the cumulative settlements as well as soil arching. According to their study, the cumulative settlement rate showed a decreasing trend with the increase of load cycle number, and the increased speed of the vehicle culminated in a faster reduction in soil arching behavior. However, Huang et al. [86] reported that the 3D numerical method, having a simple constitutive model (linear elasticity with perfect

plasticity) framework for soil, showed a satisfactory prediction of the performance of a geosynthetic-reinforced pile-supported railway embankment.

Zhuang et al. [87] also studied the load transfer process in geogrid-reinforced pile-supported embankment subjected to cyclic loading and unloading conditions, focusing mainly on the evaluation of the settlement of these systems using ABAQUS. Their study used a linear elasticity with a perfect plasticity concept with the Mohr–Coulomb material model for the embankment fill; the modified cam-clay model for the soft subsoil; and the linear elasticity concept for the geogrid, pavement, and piles in the constitutive model to simulate the complex behavior during load cycles. The authors observed that the maximum settlement at the embankment base increased by 23–55% under cyclic loading conditions but slightly rebounded under unloading, compared to the findings under static loading. Their findings demonstrated that the vertical stress rebound phenomenon occurred during cyclic loading and unloading. They also reported that this phenomenon was predominant with the variation of traffic load.

### 2.2.2. Use of Discrete Element Approach

Alternatively, discrete element modeling (DEM) is a computational approach used for solving mathematical problems related to the material having discrete characteristics, such as granular material or many other geomaterials such as soils, rocks, and aggregates [88–90]. While continuum models concentrate on constitutive rules, DEM concentrates on interaction laws [91].

Williams et al. [92] demonstrated that DEM is the simplified form of finite elements. Gaoxiao et al. [93] and Han et al. [94] used DEM and experimental procedures to analyze soil arching's mechanical properties under dynamic loads. They demonstrated that soil arching failure depends on the loading amplitude and the embankment height—the time needed for the arching collapse dramatically rose with the embankment's thickness, while with the loading amplitude, the possibility of soil arching failure increased.

Numerous researchers have used DEM to analyze the performance of different types of railway embankments (e.g., [95,96]). Han and Bhandari [97] studied geogrid-reinforced piled embankment performance subjected to cyclic loading with DEM. They reported that under cyclic loading conditions, the geogrid minimizes the embankment's vertical deformation. In particular, geogrid's inclusion provided a deformation reduction of about 25% in comparison with the unreinforced embankment while also amplifying the stress concentration ratio (the ratio between the pile top stress and the stress on the surrounding soil). The authors also mentioned that geogrid reinforcement is responsible for constant deformation after 25 cycles of load, whereas unreinforced embankment deformation showed an increasing trend with the increase of load cycles. They further identified that cyclic loading's influence principally relies upon the embankment height, pile spacing, and footing dimension.

Han et al. [98] also used DEM to investigate the stresses and deformations in geosynthetic-reinforced piled embankments. The authors concluded that geogrid in the piled embankment considerably reduced both the differential and total settlements at the embankment top. According to Lai et al. [99], although geogrid can enhance the performance of load transfer and improve the stability of soil arching, the existence of geogrid does not affect the soil's failure mode arching under the surcharge. Nonetheless, Lai et al. [100] stated that the inclusion of geosynthetics has a marginal impact on the features and formation of soil arching if the pile–subsoil relative displacement is the same for both reinforced and unreinforced situations. The authors also reported that the embankment fill's friction coefficient has a marginal impact on soil arching features and formation, even though it significantly influences the degree of soil arching effect. According to their study, embankment height controls the formation and features of soil arching. Their study also indicated that the piles' spacing significantly influences soil arching formation, but not on its features.

Nevertheless, each numerical method has some limitations regarding modeling the complex behavior of railway embankments subjected to cyclic loading, as discussed below.

### 2.3. Comparison of Modeling Approaches

The crucial problem involved in the use of continuum methods for the simulation of granular substances is the correct formulation of constitutive behavior [101]. Since granular substance micromechanics can be accurately modeled with discrete methods, an ideal adaptation of these approaches is required to model discontinuous substances' flow and displacements. However, inter-particle friction and cohesion on the microscale are usually not equivalent to the internal friction angle and cohesion, which can be measured in the laboratory on the macroscale [102]. Moreover, macroscopic quantities are reliant on the shape of the particles, internal structure, and individual movement of the particles, which is a challenging task to model and measure using DEM [103]. Furthermore, a significant amount of computational time is required to model materials in DEM.

In the case of pile-supported embankments for ballasted rail tracks, Shao et al. [104] stated that ballast, sub-ballast, embankment, and the pile foundation are all viewed as a matrix of various material parameters determined from experiments and often treated as a continuum. Research studies on FEM give a macroscopic view of ballasted railway tracks' complex behavior, according to the authors. Nevertheless, the ballast layer generally consists of a significant number of discrete elements. The ballast particles show a complicated hierarchical activity during the contact and breakage under traffic loading [104]. Consequently, the DEM is suitable for modeling the ballast aggregates as it is an efficient tool for numerical simulation of discrete particles. In contrast, continuum-based computational approaches are better suited to analyze the insights of soft soil lateral deformations, settlements, stresses, and strain rate-dependent behavior at the macroscopic scale [105]. The relationship of ballast with its substructure is an association between granular media and continuous framework [104].

When piled embankments for transport infrastructure are considered, the most common loads include gravity, hydrostatic loading (undrained analysis), and the pressure loads on the embankment, including surcharge loading and traffic loading [106]. Pham [48] observed that the geosynthetic-reinforced, pile-supported rail embankment system reduces the embankment and soft soil settlements induced by static loading up to about 5% as compared to the piled embankment without geosynthetic reinforcement. This researcher also demonstrated that the hypo-plasticity model simulates the geosynthetic-reinforced pile-supported embankment's cyclic response appropriately, as it can address the decrease of arching effect and the cumulative settlements with the increasing number of load cycles. However, yielding, strain-hardening, and strain-softening behavior, which are hard to incorporate in the continuum approach, can be easily accommodated in the DEM using the fundamental principles of packing density, coefficient of friction between the granular particles, as well as normal and shear stiffness of the particles [97]. Han and Bhandari [97] also observed that geosynthetic-reinforced, pile-supported embankment reduces the permanent deformation (by about 25%) during cyclic loading as compared to the unreinforced piled embankment, which is consistent with the results obtained by Pham [48] using the continuum approach.

Since FEM and DEM simulations are suitable for macroscopic and discrete matters, respectively, the combination of DEM and FEM can be an effective solution to address these problems, where FEM is used to model the continuum structure, and DEM is used for discrete materials [104].

The concept of coupling discrete and continuum methods to study the load-deformation behavior of pile-supported embankments, track substructure, and pavements has already been established in various forms in recent times [64,98,104,107–111]. In this coupled modeling approach, a granular layer that is governed by the interaction of discrete aggregates is usually modeled by the DEM, which is then incorporated into a continuum mechanics approach such as the FEM to analyze the surrounding soil that has a much larger domain area. Principally, coupling between the DEM and FEM zones is achieved by (i) applying the forces acting on the discrete particles as force boundary conditions to the finite element

grids, and then (ii) treating the finite nodal displacements as velocity boundary conditions (i.e., displacements) for the discrete particles.

In order to implement the above-mentioned coupling approach, the following three sequential steps are normally adopted: (i) DEM model is first generated and cycled to bring the model to initial equilibrium; (ii) a continuum mesh is then created in FEM zone to model the surrounding soil with its geometry and an appropriate constitutive model; (iii) once the setup process is completed, the coupled DEM–FEM model begins to execute in both codes, with contact forces transferred from DEM to FEM, and displacements transferred from FEM to DEM as boundary conditions via the socket I/O. It is important to note that cycling in both codes must be synchronized using the same time step ( $\Delta t$ ) so that the same displacements are calculated in both codes at each time step [112], as illustrated in Figure 10.

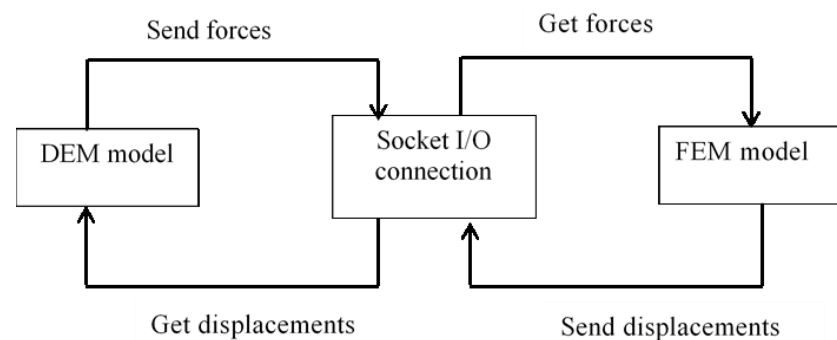


**Figure 10.** Force–displacement exchange in a coupled discrete element modeling (DEM)–finite element modeling (FEM) approach through socket I/O connection (modified after [111]).

Indraratna et al. [111] developed a coupled discrete–continuum model to study the deformation of a single stone column installed in soft ground. In this case, a mathematical framework was developed to implement the coupling mechanism (i.e., force–displacement exchange) at the interface. The model was then used to investigate the contact force distributions, the shear stress contours, and bulging developed in the stone column and surrounding clay.

Shi et al. [110] applied a coupled DEM–FEM approach to model a multi-layer railway ballast track subjected to moving wheel loads. This model was validated with both laboratory and field test data, and the authors concluded that the coupled model can provide more reliable responses compared to a purely macro-mechanical or continuum behavior of a ballast layer under a moving load.

Ngo et al. [113] developed an advanced coupled model to study the load–deformation response of the ballast layer subjected to cyclic train loading. In this study, non-uniform sizes and irregular ballast shapes were simulated in DEM by connecting a specified number of spheres clumped together to represent realistic angularity and sizes of ballast aggregates. A series of thin interface elements could then be introduced to facilitate the force–displacement exchanges. The coupled model was validated by the laboratory test data and was then used to predict the load–displacement responses of a fully instrumented rail track in the town of Singleton north of Sydney, where two types of subgrade (e.g., soft alluvial foundation and hard concrete bridge deck) were analyzed with acceptable accuracy compared to measured field data.

Adopting the above-described concepts and numerical advances, Tran et al. [64] very recently developed a coupled discrete–continuum model to study the load transfer mechanism of a geosynthetic-reinforced piled embankment, capturing the interaction between granular materials and geotextiles. In summary, the coupled discrete–continuum model is a promising numerical scheme for modelling pile-supported embankments as it fully utilizes both numerical approaches with acceptable computational effort and reasonable accuracy.



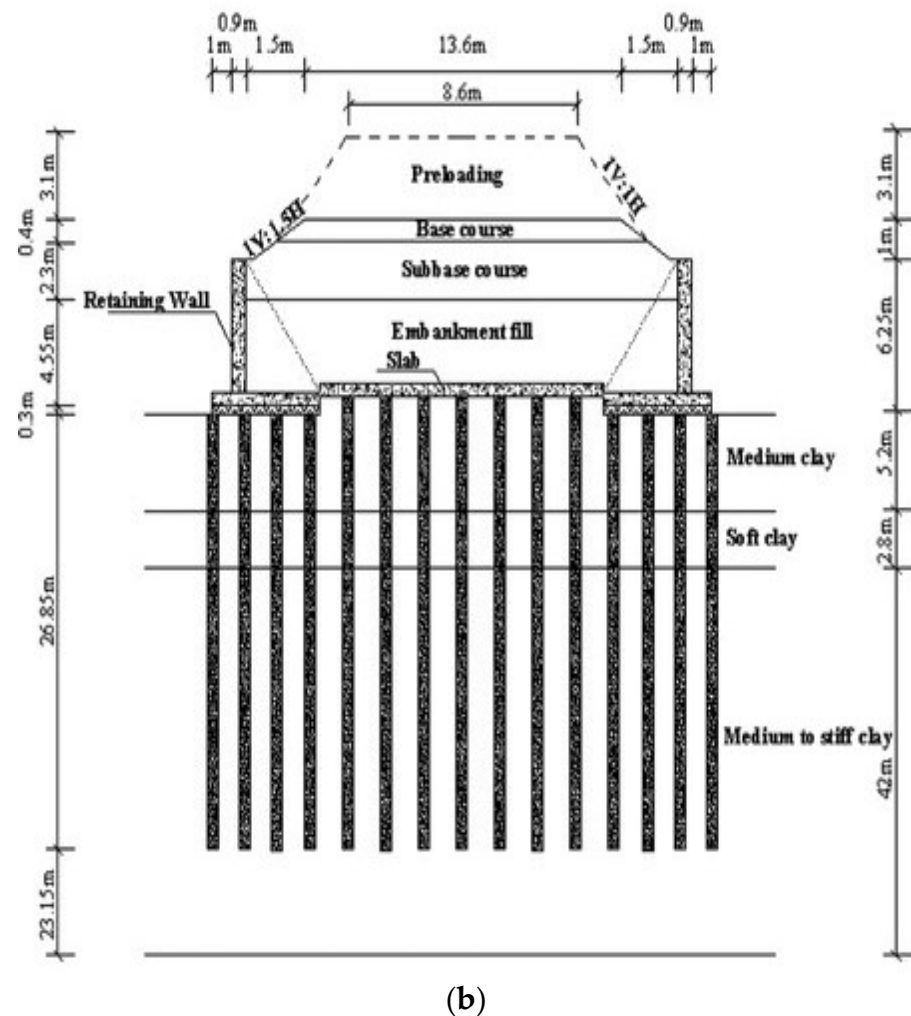


**Figure 11.** Schematic view of the embankments' cross-section: (a) Station 1, (b) Station 2 (from [118], reprinted by permission of Taylor and Francis Ltd., Abingdon, UK).

Han et al. [119] examined the soil arching behavior in geosynthetic-reinforced piled embankments of different heights under dynamic load by performing model tests and numerical simulations following Chinese high-speed railways. According to their analysis, the dynamic load directly influences the soil arching behavior when the embankment height is not high enough. They performed the model tests under two different conditions (without a geogrid and subsoil) to analyze soil arching behavior under dynamic load. The test system comprised a cylinder, an iron base with a hole, a signal acquisition system, a vibration exciter, and dynamic soil stress transducers (SSTs), as shown in Figure 12. Toughened glass was used for the cylinder wall to observe the mechanisms. The authors observed that when the embankment height exceeded the hole diameter three times, the dynamic load effects on the soil arching behavior were not predominant. On the other hand, in numerical analysis (finite element modeling), due to the presence of geogrid, when the height of the embankment exceeded 1.4 times the spacing of piles, the effect of dynamic load on the soil arching behavior was negligible, which suggests that the presence of a geogrid and subsoil will increase the stability of the soil arching during dynamic load.

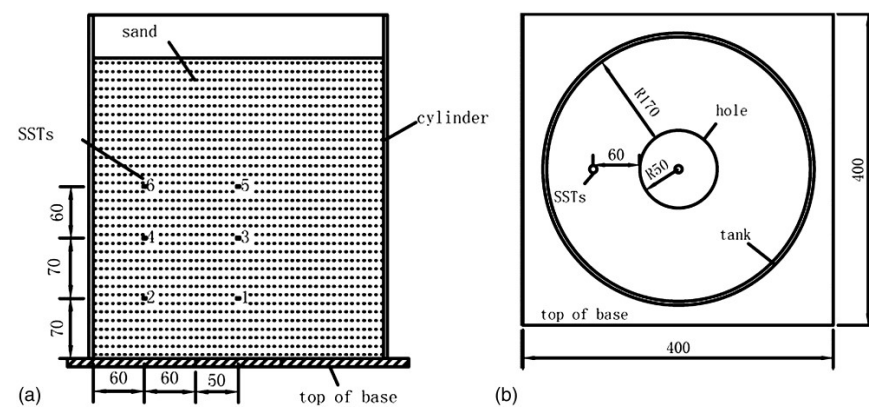


**Figure 12.** (a) Elevation and (b) planform of the test setup (all units in millimeters) (republished with permission of ASCE, from [119]; permission conveyed through Copyright Clearance Center, Inc.).

Briançon and Simon [120] studied the field performance of a pile-supported embankment with an enlarged pile head and a geosynthetic-reinforced, pile-supported embankment (i.e., an alternative solution to replace the enlarged pile head with geogrids) within the framework of the new South Europe Atlantic high-speed railway line project (Figure 13). The instrumentation's overall accuracy was checked by comparing the measurement data at identical locations recorded by different sensors. However, these sensors were unable to provide accurate measurements, mainly because of the difficulties in measuring an actual construction project. They observed that the performance of both reinforcements was identical. After consideration of all the parameters, a geosynthetic reinforcement solution was adopted for the project. This research showed that it is possible to refine a pre-designed reinforcement solution and verify the feasibility and design approach of the piling technique using full-scale experimentation.

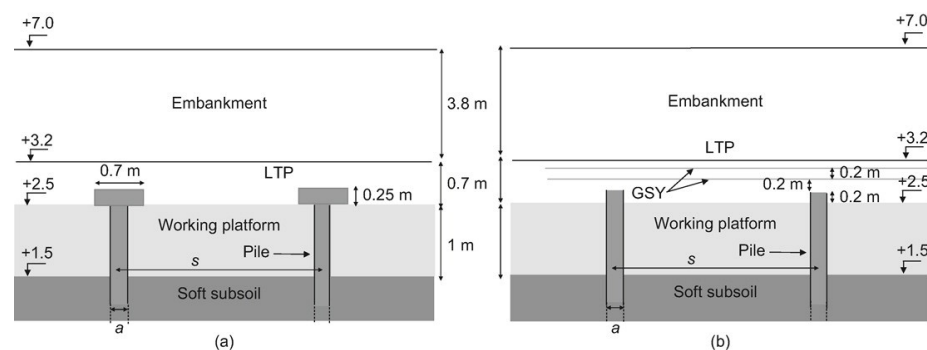


**Figure 13.** Schematic presentation of (a) piled embankment and (b) geosynthetic-reinforced piled embankment (note: LTP and GSY denote load transfer platform and geosynthetic, respectively) (republished with permission of ICE Publishing, from [120]; permission conveyed through Copyright Clearance Center, Inc.).

Wheeler et al. [121] evaluated the field performance of helical screw pile-supported peat railway subgrade located on the CN Rail Lévis subdivision in southeastern Quebec. The piles were mounted with strain gauges to determine the corresponding axial strains, piezometers were placed in the peat to monitor static and dynamic pore water pressures before and after installation of the piles, and track and subgrade displacements were measured using high-speed cameras before and after installation of the piles. A laboratory-derived conversion factor was used to convert axial strain to axial load carried by the piles. Some of the strain gauges were damaged during installation, which affected the collected pile strain data. Because of the loose peat base on-site, the cameras used to assess track displacement experienced shaking owing to ground vibrations. A potentiometer was used to evaluate the track's dynamic displacement and temperature. However, the

potentiometer only assessed track displacement data for a few weeks after installation before malfunctioning due to harsh field conditions. A vibrating wire settlement gauge was installed at a depth of 1.4 m in the sub-ballast layer. Geophones were mounted on either side of the instrumented section and used as triggers to capture the dynamic data when trains approached.

A decrease in both the excess pore pressure and the tie displacement caused by moving trains was expected after pile installation on the basis of the calculated load borne by the piles. However, it was difficult to relate the changes in pore pressure to the installation of the piles due to the post-pile data being from the months with the most significant seasonal variations. As opposed to the effect of seasonal fluctuations in both static and dynamic excess pore pressure, the piles' influence on excess pore-water pressure was not discernible. Track support system deformations revealed no significant difference between pre- and post-pile installation. Due to the limited results available, no relationship could be established between the pile's orientation and the amount of axial load borne. On the basis of the monitoring data at this location, it appeared that the expected load transfer from the ties to the piles by arching within the ballast layer was not accomplished [121].

Wang et al. [122] performed a full-scale model analysis of soil stress variations in a geosynthetic-reinforced piled railway foundation at varying water levels and loading cycles. A schematic diagram of this model is illustrated in Figure 14. Four test procedures were adopted in this study: rising of water level, lowering of water level, and cyclic loading at high and low water levels. The authors found that when the water level was lowered and the model was loaded at a low water level, the soil arching effect stayed constant, with slightly altered dynamic stresses in the railway track bed. Conversely, as the water level was raised and the loading cycles increased at a high-water level, the soil arching effect became more noticeable until the dynamic stress concentration ratio's ultimate value was achieved. They also observed that the dynamic stress above the water bag or the pile cap was barely affected by the geogrid due to the minor variance of the geogrid's transient deformation during cyclic loading.

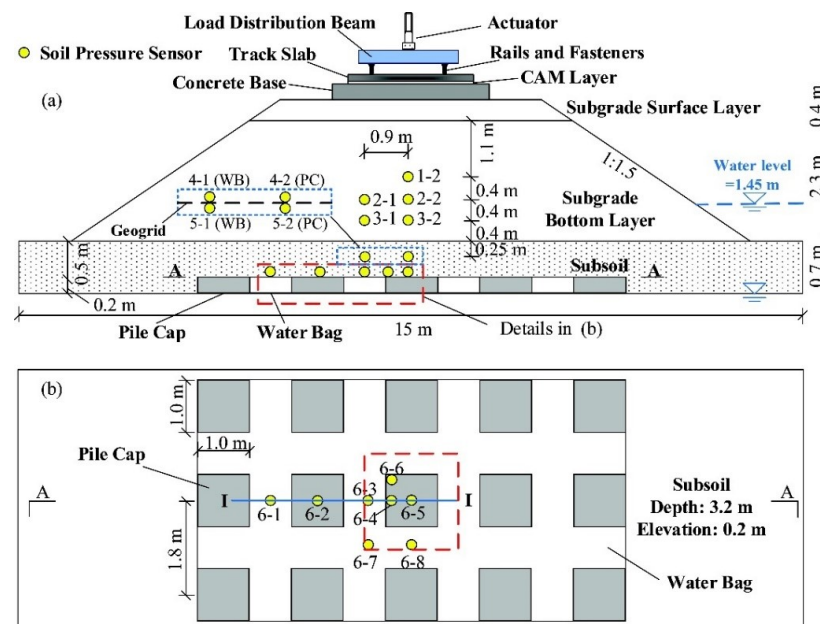


**Figure 14.** (a) Profile and (b) plan view of the testing model (from [122], Copyright Canadian Science Publishing (Ottawa, ON, Canada) or its licensors).

However, field testing may be exceedingly time-consuming, and the expenses associated with the installation of equipment, construction, and monitoring of full-scale trial embankments to determine the efficiency of various strengthening systems are usually too high to be practically sustainable [123–125].

#### 4. Research Gaps and Recommendations

As per the available literature, most of the studies on piled embankments for railway infrastructure have focused on the short-term cyclic loading effects and have not considered the time-dependent behavior of these embankments under cyclic loading. Although the system response (e.g., membrane effect in geosynthetic reinforcement and soil arching behavior) under static loading conditions is currently well known, the long-term cyclic loading behavior is not fully understood yet. Prediction of long-term differential settlement of the piled railway subgrade after millions of load cycles is necessary. Nevertheless, the numerical methods' prediction accuracy is considerably affected by the constitutive model of materials and parameters selection. Therefore, there is a need for developing an advanced model considering the aforementioned issues to make it applicable to all types of soils.

As existing literature has focused on the effects of triangular and square arrangements of piles, there is scope for further studies to investigate the effectiveness of load transfer in pile-supported rail embankments considering different pile arrangements (for example, hexagonal, circular, and rectangular patterns).

The post-construction settlement is another crucial issue often ignored in past studies, sometimes difficult to control in several regions of the world, which seriously threatens high-speed trains' operation safety. Consequently, the geometry along the track's length may deteriorate to an unacceptable degree due to undesirable settlement in the soft soils. Therefore, an in-depth study on the post-construction effect is needed considering different geometric sizes and shapes of piles to ensure high-speed trains' safe and efficient operation.

The railway track's differential settlement mainly appears in regions of foundation non-uniformities, transitions between different substructures due to structural differences, and connections between foundation treatment sections. Since most researchers have overlooked these vital issues, they should thus be addressed in future studies. Furthermore, the effect of pile-net structure on low railway embankments in soft soil areas under cyclic loading is another topic that deserves further investigation.

Most importantly, reducing calculation time with prediction accuracy should be a prime concern in future studies based on large-scale field trials using advanced user subroutines in sophisticated numerical models.

#### 5. Conclusions

The traditional ballasted railway track is the earliest type of railway pathway introduced in the world and one of the most commonly used. Superstructure (including rails, sleepers or ties, rail pads, and fasteners) and substructure (including ballast, sub-ballast, and subgrade) are the two main components of the ballasted railway lines. Rail routes over problematic subgrades, comprising soft, porous, expansive, and collapsible soils, have the potential for undesirable settlement subjected to vertical loads and mobilization of low load-carrying capacity. During their operation period, the railway embankments typically face a wide range of cyclic loads. Consequently, special attention has to be given to rail beds overlying these troublesome soils, which is time-consuming and represents a high operational cost.

Piles are gradually being used as a cost-effective and environmentally sustainable alternative to increase the bearing capacity of soft soils underlying rail embankments. Therefore, a detailed analysis is required to understand the fundamental processes and effect of pile installation on rail embankments subjected to cyclic loading. However, field testing is often time-consuming and the construction and monitoring costs of full-scale trial embankments are generally too high to be practically sustainable.

Numerical approaches such as FEM and DEM have increasingly been used due to computing technology advancements to predict embankment behavior as per the available literature. With sufficient computing time, FEM can efficiently model the whole railway network. FEM is one of the best computational methods for exploring the macroscopic behavior of a ballasted railway system. The main challenge involved in using the

FEM technique is to select a suitable material model to simulate the complex behavior of the materials.

Alternatively, DEM is used to address the mathematical problems related to discrete matters. Compared to the FEM, DEM models every particle as an independent body and depicts granular substances as idealized particle assembly. This method is applicable for validating experimental procedures for small-scale models. Macroscopic amounts are dependent on the form of objects, the internal composition, and the individual movement of the objects, which is a challenging task to model and measure using DEM. Moreover, a large amount of computational time is required to accomplish the designated task using DEM.

The combination of DEM and FEM can be an effective solution to model pile-supported railway embankments under cyclic loading. In this coupled model, DEM is used to simulate the discrete ballast grains, whereas the FEM is used to simulate the subgrade domain as a continuum. This coupled approach's main benefits arise from the combination of the advantages of both the FEM and DEM and the possibility of simulating the continuum structure and the discrete materials, as well as the interaction between these components.

Furthermore, an advanced numerical model with user subroutines should be introduced to minimize the calculation time and increase prediction accuracy considering practical problems in the field.

**Author Contributions:** Conceptualization and writing—original draft preparation, A.S.M.R.; supervision and writing—review and editing, F.B.F. and B.I.; writing—review and editing, T.N. All authors have read and agreed to the published version of the manuscript.

**Funding:** This work was financially supported by: Programmatic funding—UIDP/04708/2020 of the CONSTRUCT—Instituto de I&D em Estruturas e Construções—funded by national funds through the FCT/MCTES (PIDDAC).

**Informed Consent Statement:** Not applicable.

**Data Availability Statement:** Not applicable.

**Acknowledgments:** A substantial portion of the technical content of this paper has been reproduced from past literature for the main purpose of review. In accordance, the Authors are grateful to the original sources for granting them permission to reproduce the appropriate artwork/Figures and data in this review paper. The support from UTS Transport Research Centre is also gratefully acknowledged.

**Conflicts of Interest:** The authors declare no conflict of interest.

## References

1. Berggren, E. Railway Track Stiffness: Dynamic Measurements and Evaluation for Efficient Maintenance. Ph.D. Thesis, Royal Institute of Technology (KTH), Aeronautical and Vehicle Engineering, Division of Rail Vehicles, Stockholm, Sweden, 8 May 2009.
2. Indraratna, B.; Salim, W.; Christie, D. Improvement of Recycled Ballast Using Geosynthetics. Geosynthetics—State of the Art—Recent Developments. In Proceedings of the 7th International Conference on Geosynthetics, Nice, France, 22–27 September 2002; Delmas, P.H., Gourc, J.P., Girard, H., Eds.; Balkema: Lisse, The Netherlands, 2002; pp. 1177–1182.
3. Ionescu, D.; Indraratna, B.; Christie, H.D. Behaviour of Railway Ballast under Dynamic Loads. In Proceedings of the 13th Southeast Asian Geotechnical Conference, Taipei, Taiwan, 16–20 November 1998; pp. 69–74.
4. Wheat, P.; Smith, A.S. Assessing the Marginal Infrastructure Maintenance Wear and Tear Costs for Britain's Railway Network. *J. Transp. Econ. Policy* **2008**, *42*, 189–224.
5. Indraratna, B.; Ngo, T.; Rujikiatkamjorn, C. Performance of Ballast Influenced by Deformation and Degradation: Laboratory Testing and Numerical Modeling. *Int. J. Géoméch.* **2020**, *20*, 04019138. [[CrossRef](#)]
6. Indraratna, B.; Qi, Y.; Ngo, T.N.; Rujikiatkamjorn, C.; Neville, T.; Ferreira, F.B.; Shahkolahi, A. Use of Geogrids and Recycled Rubber in Railroad Infrastructure for Enhanced Performance. *Geosciences* **2019**, *9*, 30. [[CrossRef](#)]
7. Indraratna, B.; Ferreira, F.B.; Qi, Y.; Ngo, T.N. Application of geoinclusions for sustainable rail infrastructure under increased axle loads and higher speeds. *Innov. Infrastruct. Solut.* **2018**, *3*, 69. [[CrossRef](#)]
8. Kaewunruen, S.; Remennikov, A.M. Dynamic properties of railway track and its components: Recent findings and future research direction. *Insight Non-Destr. Test. Cond. Monit.* **2010**, *52*, 20–22. [[CrossRef](#)]
9. Ferreira, F.; Indraratna, B. Deformation and Degradation Response of Railway Ballast under Impact Loading—Effect of Artificial Inclusions. In Proceedings of the 1st International Conference on Rail Transportation, Chengdu, China, 10–12 July 2017; ASCE: Reston, VA, USA, 2018; pp. 1090–1101. [[CrossRef](#)]

10. Hussaini, S.K.K.; Indraratna, B.; Vinod, J.S. A laboratory investigation to assess the functioning of railway ballast with and without geogrids. *Transp. Geotech.* **2016**, *6*, 45–54. [[CrossRef](#)]
11. Indraratna, B.; Ngo, T.; Ferreira, F.B.; Rujikiatkamjorn, C.; Shahkolahi, A. Laboratory examination of ballast deformation and degradation under impact loads with synthetic inclusions. *Transp. Geotech.* **2020**, *25*, 100406. [[CrossRef](#)]
12. Indraratna, B.; Sun, Q.; Grant, J. Behaviour of subballast reinforced with used tyre and potential application in rail tracks. *Transp. Geotech.* **2017**, *12*, 26–36. [[CrossRef](#)]
13. Indraratna, B.; Salim, W. *Mechanics of Ballasted Rail Tracks: A Geotechnical Perspective*; Taylor & Francis: London, UK, 2005.
14. Jayasuriya, C.; Indraratna, B.; Ngo, T.N. Experimental study to examine the role of under sleeper pads for improved performance of ballast under cyclic loading. *Transp. Geotech.* **2019**, *19*, 61–73. [[CrossRef](#)]
15. Liu, C.; Ngo, N.T.; Indraratna, B. Improved performance of railroad ballast using geogrids. In *Lecture Notes in Civil Engineering, Geotechnics for Transportation Infrastructure*; Sundaram, R., Shahu, J., Havanagi, V., Eds.; Springer: Singapore, 2019; Volume 29, pp. 151–163. [[CrossRef](#)]
16. Navaratnarajah, S.K.; Indraratna, B.; Ngo, N.T. Influence of under Sleeper Pads on Ballast Behavior Under Cyclic Loading: Experimental and Numerical Studies. *J. Geotech. Geoenviron. Eng.* **2018**, *144*, 04018068. [[CrossRef](#)]
17. Nimbalkar, S.; Dash, S.K.K.; Indraratna, B. Performance of Ballasted Track under Impact Loading and Applications of Recycled Rubber Inclusion. *Geotech. Eng.* **2018**, *49*, 79–91.
18. Ngo, N.T.; Indraratna, B. Interface behavior of geogrid-reinforced sub-ballast: Laboratory and discrete element modeling. In *Lecture Notes in Civil Engineering, Geotechnics for Transportation Infrastructure*; Sundaram, R., Shahu, J., Havanagi, V., Eds.; Springer: Singapore, 2019; Volume 29, pp. 195–209. [[CrossRef](#)]
19. Ngo, N.T.; Indraratna, B.; Ferreira, F.B.; Rujikiatkamjorn, C. Improved performance of geosynthetics enhanced ballast: Laboratory and numerical studies. *Proc. Inst. Civ. Eng. Ground Improv.* **2018**, *171*, 202–222. [[CrossRef](#)]
20. Ngo, N.T.; Indraratna, B.; Rujikiatkamjorn, C. A study of the geogrid–subballast interface via experimental evaluation and discrete element modelling. *Granul. Matter* **2017**, *19*, 54. [[CrossRef](#)]
21. Ngo, N.T. Dem Modelling of Geocell-Stabilised Sub-Ballast under Cyclic Loading. *Int. J. GEOMATE* **2017**, *12*, 23–29. [[CrossRef](#)]
22. Ngo, N.T.; Indraratna, B.; Rujikiatkamjorn, C.; Biabani, M.M. Experimental and Discrete Element Modeling of Geocell-Stabilized Subballast Subjected to Cyclic Loading. *J. Geotech. Geoenviron. Eng.* **2016**, *142*, 04015100. [[CrossRef](#)]
23. López-Pita, A.; Teixeira, P.F.; Casas, C.; Bachiller, A.; Ferreira, P.A. Maintenance Costs of High-Speed Lines in Europe State of the Art. *Transp. Res. Rec. J. Transp. Res. Board* **2008**, *2043*, 13–19. [[CrossRef](#)]
24. Puppala, A.J.; Madhyannapu, R.S.; Nazarian, S.; Yuan, D.; Hoyos, L. *Deep Soil Mixing Technology for Mitigation of Pavement Roughness*; Report No. FHWA/TX-08/0-5179-1; The University of Texas: Arlington, TX, USA, 2008.
25. Indraratna, B.; Chu, J.; Rujikiatkamjorn, C. *Ground Improvement Case Histories—Embankments with Special Reference to Consolidation and other Physical Methods*; Elsevier: Cambridge, MA, USA, 2015; p. 817.
26. Brecciaroli, F.; Kolisoja, P. *Deformation Behaviour of Railway Embankment Materials under Repeated Loading: Literature Review*; Publication No. A 5/2006; Finnish Rail Administration, Rail Network Department: Helsinki, Finland, 2006.
27. Yun-Min, C.; Wei-Ping, C.; Ren-Peng, C. An experimental investigation of soil arching within basal reinforced and unreinforced piled embankments. *Geotext. Geomembr.* **2008**, *26*, 164–174. [[CrossRef](#)]
28. Jenck, O.; Dias, D.; Kastner, R. Two-Dimensional Physical and Numerical Modeling of a Pile-Supported Earth Platform over Soft Soil. *J. Geotech. Geoenviron. Eng.* **2007**, *133*, 295–305. [[CrossRef](#)]
29. Lee, C.; Wu, B.; Chen, H.; Chiang, K. Tunnel stability and arching effects during tunneling in soft clayey soil. *Tunn. Undergr. Space Technol.* **2006**, *21*, 119–132. [[CrossRef](#)]
30. Brown, S.F.; Lashine, A.K.F.; Hyde, A.F.L. Repeated load triaxial testing of a silty clay. *Géotechnique* **1975**, *25*, 95–114. [[CrossRef](#)]
31. Li, L.-L.; Dan, H.-B.; Wang, L.-Z. Undrained behavior of natural marine clay under cyclic loading. *Ocean Eng.* **2011**, *38*, 1792–1805. [[CrossRef](#)]
32. Li, D.; Selig, E.T. Cumulative Plastic Deformation for Fine-Grained Subgrade Soils. *J. Geotech. Eng.* **1996**, *122*, 1006–1013. [[CrossRef](#)]
33. Miller, G.A.; Teh, S.Y.; Li, D.; Zaman, M.M. Cyclic Shear Strength of Soft Railroad Subgrade. *J. Geotech. Geoenviron. Eng.* **2000**, *126*, 139–147. [[CrossRef](#)]
34. Seed, H.B.B.; Chan, C.K.; Monismith, C.L. Effects of repeated loading on the strength and deformation of compacted clay. In Proceedings of the 34th Annual Meeting of the Highway Research Board, Washington, DC, USA, 11–14 January 1955; Volume 34, pp. 541–558.
35. Abdullah, C.H.; Edil, T.B. Behaviour of geogrid-reinforced load transfer platforms for embankment on rammed aggregate piers. *Geosynth. Int.* **2007**, *14*, 141–153. [[CrossRef](#)]
36. Almeida, M.; Hosseinpour, I.; Riccio, M. Performance of a geosynthetic-encased column (GEC) in soft ground: Numerical and analytical studies. *Geosynth. Int.* **2013**, *20*, 252–262. [[CrossRef](#)]
37. Chen, R.; Chen, Y.M.; Han, J.; Xu, Z.Z. A theoretical solution for pile-supported embankments on soft soils under one-dimensional compression. *Can. Geotech. J.* **2008**, *45*, 611–623. [[CrossRef](#)]
38. Chen, R.P.; Xu, Z.Z.; Chen, Y.M.; Ling, D.S.; Zhu, B. Field Tests on Pile-Supported Embankments over Soft Ground. *J. Geotech. Geoenviron. Eng.* **2010**, *136*, 777–785. [[CrossRef](#)]

39. Britton, E.; Naughton, P.J. The Arching Mechanism in Piled Embankments under Road and Rail Infrastructure. *Advances in Transportation Geotechnics*. In Proceedings of the 1st International Conference on Transportation Geotechnics, Nottingham, UK, 25–27 August 2008; Ellis, E., Yu, H.-S., McDowell, G., Dawson, A., Thom, N., Eds.; Taylor & Francis: London, UK, 2008; pp. 377–381.
40. Beute, J. Problems with Cast-in-Situ Concrete Piles: A Study on the Possible Causes of Excessive Bleeding. Master's Thesis, Delft University of Technology, Delft, The Netherlands, 13 January 2020.
41. Qi, Y.; Indraratna, B. Energy-Based Approach to Assess the Performance of a Granular Matrix Consisting of Recycled Rubber, Steel-Furnace Slag, and Coal Wash. *J. Mater. Civ. Eng.* **2020**, *32*, 04020169. [[CrossRef](#)]
42. Hughes, J.; Withers, N. Reinforcing of soft cohesive soils with stone columns. *Ground Eng.* **1974**, *7*, 42–49. [[CrossRef](#)]
43. Hughes, J.M.O.; Withers, N.J.; Greenwood, D.A. A field trial of the reinforcing effect of a stone column in soil. *Géotechnique* **1975**, *25*, 31–44. [[CrossRef](#)]
44. Madhav, M.R.; Vitkar, P.P. Strip footing on weak clay stabilized with a granular trench or pile. *Can. Geotech. J.* **1978**, *15*, 605–609. [[CrossRef](#)]
45. Radjai, F.; Azéma, E. Shear strength of granular materials. *Eur. J. Environ. Civ. Eng.* **2009**, *13*, 203–218. [[CrossRef](#)]
46. Terzaghi, K. *Theoretical Soil Mechanics*; Wiley: New York, NY, USA, 1943; pp. 66–76.
47. Meena, N.K.; Nimbalkar, S.; Fatahi, B.; Yang, G. Effects of soil arching on behavior of pile-supported railway embankment: 2D FEM approach. *Comput. Geotech.* **2020**, *123*, 103601. [[CrossRef](#)]
48. Pham, V.H. 3D Modeling of Soft Soil Improvement by Rigid Inclusions-Complex and Cyclic Loading. Ph.D. Thesis, Université Grenoble Alpes, Grenoble, France, 17 September 2018.
49. Jenck, O.; Dias, D.; Kastner, R. Three-Dimensional Numerical Modeling of a Piled Embankment. *Int. J. Géoméch.* **2009**, *9*, 102–112. [[CrossRef](#)]
50. Van Eekelen, S.J.M.; Bezuijen, A. Dutch Research on Basal Reinforced Piled Embankments. In Proceedings of the 2013 Geo-Congress Conference, San Diego, CA, USA, 3–7 March 2013; Meehan, C., Pradel, D., Pando, M.A., Labuz, J.F., Eds.; ASCE: Reston, VA, USA, 2013; pp. 1838–1847. [[CrossRef](#)]
51. Chew, S.H.H.; Phoon, H.L.; Loke, K.H.; Lim, L.K.; Le Hello, B.; Villard, P. Geotextile Reinforced Piled Embankment-Full Scale Model Tests. In Proceedings of the 3rd Asian Regional Conference on geosynthetics, Seoul, Korea, 21–24 June 2004; Shim, J.B., Yoo, C., Jeon, H.-Y., Eds.; pp. 661–668. [[CrossRef](#)]
52. Hewlett, W.J.; Randolph, M.F. Analysis of Piled Embankments. *Ground Eng.* **1988**, *21*, 12–18.
53. Low, B.K.; Tang, S.K.; Choa, V. Arching in Piled Embankments. *J. Geotech. Eng.* **1994**, *120*, 1917–1938. [[CrossRef](#)]
54. Almeida, M.S.S.; Ehrlich, M.; Spotti, A.P.; Marques, M.E.S. Embankment supported on piles with biaxial geogrids. *Proc. Inst. Civ. Eng. Geotech. Eng.* **2007**, *160*, 185–192. [[CrossRef](#)]
55. Briançon, L.; Simon, B. Performance of Pile-Supported Embankment over Soft Soil: Full-Scale Experiment. *J. Geotech. Geoenviron. Eng.* **2012**, *138*, 551–561. [[CrossRef](#)]
56. Kempfert, H.G.; Heitz, C.; Raitel, M. Geogrid reinforced railway embankment on piles, railway Hamburg-Berlin Germany. In Proceedings of the International Conference on Geosynthetic and Geoenvironmental Engineering, IIT Bombay, Mumbai, India, 8–10 December 2004; pp. 1–6.
57. Oh, Y.I.; Shin, E.C. Reinforcement and Arching Effect of Geogrid-Reinforced and Pile-Supported Embankment on Marine Soft Ground. *Mar. Georesour. Geotechnol.* **2007**, *25*, 97–118. [[CrossRef](#)]
58. Quigley, P.; O'Malley, J.; Rodgers, M. Performance of a Trial Piled Embankment Constructed on Soft Compressible Estuarine Deposits at Shannon, Ireland. In Proceedings of the International Workshop on Geotechnics of Soft Soils: Theory and Practice, Noordwijkerhout, The Netherlands, 17–19 September 2003; pp. 619–624.
59. Sloan, J.A. Column-Supported Embankments: Full-Scale Tests and Design Recommendations. Ph.D. Thesis, Virginia Polytechnic Institute and State University, Blacksburg, VA, USA, 26 May 2011.
60. Wang, H.-L.; Chen, R.-P. Estimating Static and Dynamic Stresses in Geosynthetic-Reinforced Pile-Supported Track-Bed under Train Moving Loads. *J. Geotech. Geoenviron. Eng.* **2019**, *145*, 04019029. [[CrossRef](#)]
61. Zhang, L.; Zhou, S.; Zhao, H.; Deng, Y. Performance of Geosynthetic-Reinforced and Pile-Supported Embankment with Consideration of Soil Arching. *J. Eng. Mech.* **2018**, *144*, 06018005. [[CrossRef](#)]
62. Zhang, C.; Jiang, G.; Liu, X.; Buzzi, O. Arching in geogrid-reinforced pile-supported embankments over silty clay of medium compressibility: Field data and analytical solution. *Comput. Geotech.* **2016**, *77*, 11–25. [[CrossRef](#)]
63. Ferreira, P.; Maciel, R.; Estaire, J.; Rodriguez-Plaza, M. Railway track design optimisation for enhanced performance at very high speeds: Experimental measurements and computational estimations. *Struct. Infrastruct. Eng.* **2018**, *15*, 1–13. [[CrossRef](#)]
64. Tran, Q.A.; Villard, P.; Dias, D. Geosynthetic reinforced piled embankment modeling using discrete and continuum approaches. *Geotext. Geomembr.* **2021**, *49*, 243–256. [[CrossRef](#)]
65. Badakhshan, E.; Noorzad, A.; Bouazza, A.; Dafalias, Y.F.; Zameni, S.; King, L. Load recovery mechanism of arching within piled embankments using discrete element method and small scale tests. *Powder Technol.* **2020**, *359*, 59–75. [[CrossRef](#)]
66. Lai, H.-J.; Zheng, J.-J.; Cui, M.-J.; Chu, J. “Soil arching” for piled embankments: Insights from stress redistribution behaviour of DEM modelling. *Acta Geotech.* **2020**, *15*, 2117–2136. [[CrossRef](#)]
67. Ariyaratne, P.; Liyanapathirana, D.S.; Leo, C.J. Comparison of Different Two-Dimensional Idealizations for a Geosynthetic-Reinforced Pile-Supported Embankment. *Int. J. Géoméch.* **2013**, *13*, 754–768. [[CrossRef](#)]

68. Bhasi, A.; Rajagopal, K. Numerical investigation of time dependent behavior of geosynthetic reinforced piled embankments. *Int. J. Geotech. Eng.* **2013**, *7*, 232–240. [[CrossRef](#)]
69. Han, J.; Gabr, M.A. Numerical Analysis of Geosynthetic-Reinforced and Pile-Supported Earth Platforms over Soft Soil. *J. Geotech. Geoenviron. Eng.* **2002**, *128*, 44–53. [[CrossRef](#)]
70. Li, X.; Miao, Y.; Cheng, K. Soil Arching Effect Analysis via a Modified Finite Element Model Based on a Field Test. *J. Test. Eval.* **2018**, *46*, 2218–2226. [[CrossRef](#)]
71. Pham, H.; Dias, D. 3D Numerical Modeling of a Piled Embankment under Cyclic Loading. *Int. J. Géoméch.* **2019**, *19*, 04019010. [[CrossRef](#)]
72. Naughton, P.J. The Significance of Critical Height in the Design of Piled Embankments. In Proceedings of the GeoDenver 2007, New Peaks in Geotechnic, Denver, CO, USA, 18–21 February 2007; ASCE: Reston, VA, USA, 2007; pp. 13–23. [[CrossRef](#)]
73. Spangler, M.G.; Handy, R.L. *Soil Engineering*, 3rd ed.; Intext Educational Publishers: New York, NY, USA, 1973.
74. Terzaghi, K. Stress distribution in dry and in saturated sand above a yielding trapdoor. In Proceedings of the 1st International Conference on Soil Mechanics and Foundation Engineering, Cambridge, MA, USA, 22–26 June 1936; Volume 1, pp. 307–311.
75. Carlson, B.O. *Armerad Jord Beräkningsprinciper för Banker På Pålar*; Terranova, Distr. SGI: Linköping, Sweden, 1987. (In Swedish)
76. BS 8006. *Code of Practice for Strengthened/Reinforced soils and Other Fills*; British Standards Institution: London, UK, 1995.
77. Horgan, G.J.; Sarsby, R.W. The Arching Effect of Soils over Voids and Piles Incorporating Geosynthetic Reinforcement. Geosynthetics—State of the Art—Recent Developments. In Proceedings of the 7th International Conference on Geosynthetics, Nice, France, 22–27 September 2002; Delmas, P.H., Gourc, J.P., Girard, H., Eds.; Balkema: Lisse, The Netherlands, 2002; pp. 373–378.
78. Russell, D.; Naughton, P.J.; Kempton, G. A new design procedure for piled embankments. In Proceedings of the 56th Canadian Geotechnical Conference and 2003 NAGS Conference, Winnipeg, MB, Canada, 29 September–1 October 2003; Volume 1, pp. 858–865.
79. Van Eekelen, S.J.M.; Bezuijen, A.; Oung, O. Arching in Piled Embankments; Experiments and Design Calculations. In Proceedings of the BGA International Conference on Foundations: Innovations, Observations, Design and Practice, Dundee, UK, 2–5 September 2003; Newson, T.A., Ed.; Thomas Telford Publishing: London, UK, 2003; pp. 885–894.
80. Kempfert, H.G.; Gobel, C.; Alexiew, D.; Heitz, C. German recommendations for reinforced embankments on pile-similar elements. In Proceedings of the 3rd European Geosynthetics Conference, Munich, Germany, 1–3 March 2004; pp. 279–284.
81. Ariyaratne, P.; Liyanapathirana, D. Review of existing design methods for geosynthetic-reinforced pile-supported embankments. *Soils Found.* **2015**, *55*, 17–34. [[CrossRef](#)]
82. Guido, V.A.; Kneuppel, J.D.; Sweeney, M.A. Plate loading tests on geogrid reinforced earth slabs. In Proceedings of the 87 Geosynthetics Conference, New Orleans, LA, USA, 24–25 February 1987; pp. 216–225.
83. BS 8006. *Code of Practice for Strengthened/Reinforced Soils and Other Fills*; British Standards Institution: London, UK, 2010.
84. Nunez, M.; Briançon, L.; Dias, D.C.F.S. Analyses of a pile-supported embankment over soft clay: Full-scale experiment, analytical and numerical approaches. *Eng. Geol.* **2013**, *153*, 53–67. [[CrossRef](#)]
85. Pham, H.; Dias, D.; Dudchenko, A. 3D modeling of geosynthetic-reinforced pile-supported embankment under cyclic loading. *Geosynth. Int.* **2020**, *27*, 157–169. [[CrossRef](#)]
86. Huang, J.; Han, J.; Collin, J.G. Geogrid-Reinforced Pile-Supported Railway Embankments. *Transp. Res. Rec.* **2005**, *1936*, 221–229. [[CrossRef](#)]
87. Zhuang, Y.; Cui, X.; Zhang, S.; Dai, G.; Zhao, X. The load transfer mechanism in reinforced piled embankment under cyclic loading and unloading. *Eur. J. Environ. Civ. Eng.* **2020**, 1–15. [[CrossRef](#)]
88. Mohammadinia, A.; Oskoei, P.R.; Arulrajah, A. Discrete element modeling of cemented recycled concrete aggregates under unconfined and k0 loading conditions. *Transp. Geotech.* **2021**, *26*, 100450. [[CrossRef](#)]
89. Arulrajah, A.; Baghban, H.; Narsilio, G.A.; Horpibulsuk, S.; Leong, M. Discrete element analysis of recycled concrete aggregate responses during repeated load triaxial testing. *Transp. Geotech.* **2020**, *23*, 100356. [[CrossRef](#)]
90. Xu, W.-J.; Wang, S.; Zhang, H.-Y.; Zhang, Z.-L. Discrete element modelling of a soil-rock mixture used in an embankment dam. *Int. J. Rock Mech. Min. Sci.* **2016**, *86*, 141–156. [[CrossRef](#)]
91. Mahabadi, O.K.; Lisjak, A.; Munjiza, A.; Grasselli, G. Y-Geo: New Combined Finite-Discrete Element Numerical Code for Geomechanical Applications. *Int. J. Géoméch.* **2012**, *12*, 676–688. [[CrossRef](#)]
92. Williams, J.R.; Hocking, G.; Mustoe, G.G.W. The Theoretical Basis of the Discrete Element Method. In Proceedings of the International Conference on Numerical Methods in Engineering: Theory and Applications, Swansea, UK, 7–11 January 1985; Middleton, J., Pande, G.N., Eds.; Balkema: Rotterdam, The Netherlands, 1985; pp. 897–906.
93. Gaoxiao, H.; Quanmei, G.; Shunhua, Z. Mechanical Analysis of Soil Arching under Dynamic Loads. In Proceedings of the Pan-Am CGS Geotechnical Conference, Toronto, ON, Canada, 2–6 October 2011; pp. 2996–3002.
94. Han, G.-X.; Gong, Q.-M.; Zhou, S.-H. An Experimental Investigation of Soil Arching under Dynamic Loads. In Proceedings of the 11th International Conference of Chinese Transportation Professionals (ICCTP), Nanjing, China, 14–17 August 2011; ASCE: Reston, VA, USA, 2012; pp. 3030–3037. [[CrossRef](#)]
95. Lopez, R.D.F.; Larsson, S.; Silfwerbrand, J. A discrete element material model including particle degradation suitable for rockfill embankments. *Comput. Geotech.* **2019**, *115*, 103166. [[CrossRef](#)]

96. Gu, Q.; Bian, X.; Morrissey, J.P. DEM Simulation of Simplified Railway Embankment Under the Effect of Train-Induced Dynamic Load. In Proceedings of the 7th International Symposium on Environmental Vibration and Transportation Geodynamics, Hangzhou, China, 28–30 October 2016; Bian, X., Chen, Y., Ye, X., Eds.; Springer: Singapore, 2016; pp. 423–431. [\[CrossRef\]](#)
97. Han, J.; Bhandari, A. Evaluation of Geogrid-Reinforced Pile-Supported Embankments under Cyclic Loading Using Discrete Element Method. *Adv. Ground Improv.* **2009**, *73*–82. [\[CrossRef\]](#)
98. Han, J.; Bhandari, A.; Wang, F. DEM Analysis of Stresses and Deformations of Geogrid-Reinforced Embankments over Piles. *Int. J. Géoméch.* **2012**, *12*, 340–350. [\[CrossRef\]](#)
99. Lai, H.-J.; Zheng, J.-J.; Zhang, J.; Zhang, R.-J.; Cui, L. DEM analysis of “soil”-arching within geogrid-reinforced and unreinforced pile-supported embankments. *Comput. Geotech.* **2014**, *61*, 13–23. [\[CrossRef\]](#)
100. Lai, H.J.; Zheng, J.J.; Zhang, R.J.; Cui, M.J. Visualization of the Formation and Features of Soil Arching within a Piled Embankment by Discrete Element Method Simulation. *J. Zhejiang Univ. Sci. A* **2016**, *17*, 803–817. [\[CrossRef\]](#)
101. Weinhart, T.; Thornton, A.R.; Einav, I. Editorial: Modelling and computational challenges in granular materials. *Comput. Part. Mech.* **2015**, *3*, 291–292. [\[CrossRef\]](#)
102. Yang, Z.X.; Yang, J.; Wang, L.Z. On the influence of inter-particle friction and dilatancy in granular materials: A numerical analysis. *Granul. Matter* **2012**, *14*, 433–447. [\[CrossRef\]](#)
103. Radjai, F.; Roux, J.-N.; Daouadji, A. Modeling Granular Materials: Century-Long Research across Scales. *J. Eng. Mech.* **2017**, *143*, 04017002. [\[CrossRef\]](#)
104. Shao, S.; Yan, Y.; Ji, S. Combined Discrete–Finite Element Modeling of Ballasted Railway Track Under Cyclic Loading. *Int. J. Comput. Methods* **2016**, *14*, 1750047. [\[CrossRef\]](#)
105. Indraratna, B.; Ngo, N.T.; Rujikiatkamjorn, C. Behavior of geogrid-reinforced ballast under various levels of fouling. *Geotext. Geomembr.* **2011**, *29*, 313–322. [\[CrossRef\]](#)
106. Zhuang, Y.; Li, S. Three-dimensional finite element analysis of arching in a piled embankment under traffic loading. *Arab. J. Geosci.* **2015**, *8*, 7751–7762. [\[CrossRef\]](#)
107. Dratt, M.; Katterfeld, A. Coupling of FEM and DEM simulations to consider dynamic deformations under particle load. *Granul. Matter* **2017**, *19*, 1–15. [\[CrossRef\]](#)
108. Guo, N.; Zhao, J. A coupled FEM/DEM approach for hierarchical multiscale modelling of granular media. *Int. J. Numer. Methods Eng.* **2014**, *99*, 789–818. [\[CrossRef\]](#)
109. O’Sullivan, C. *Particulate Discrete Element Modelling: A Geomechanics Perspective*; Spon Press: London, UK, 2011.
110. Shi, C.; Zhao, C.; Zhang, X.; Guo, Y. Coupled discrete-continuum approach for railway ballast track and subgrade macro-meso analysis. *Int. J. Pavement Eng.* **2020**, 1–16. [\[CrossRef\]](#)
111. Indraratna, B.; Ngo, N.T.; Rujikiatkamjorn, C.; Sloan, S.W. Coupled discrete element–finite difference method for analysing the load-deformation behaviour of a single stone column in soft soil. *Comput. Geotech.* **2015**, *63*, 267–278. [\[CrossRef\]](#)
112. Itasca. *Particle Flow Code in Two and Three Dimensions*; Itasca Consulting Group, Inc.: Minneapolis, MN, USA, 2016.
113. Ngo, N.T.; Indraratna, B.; Rujikiatkamjorn, C. Simulation Ballasted Track Behavior: Numerical Treatment and Field Application. *Int. J. Géoméch.* **2017**, *17*, 04016130. [\[CrossRef\]](#)
114. Guo, L.; Xiang, J.; Latham, J.-P.; Izzuddin, B. A numerical investigation of mesh sensitivity for a new three-dimensional fracture model within the combined finite-discrete element method. *Eng. Fract. Mech.* **2016**, *151*, 70–91. [\[CrossRef\]](#)
115. Oñate, E.; Rojek, J. Combination of discrete element and finite element methods for dynamic analysis of geomechanics problems. *Comput. Methods Appl. Mech. Eng.* **2004**, *193*, 3087–3128. [\[CrossRef\]](#)
116. Villard, P.; Chevalier, B.; Le Hello, B.; Combe, G. Coupling between finite and discrete element methods for the modelling of earth structures reinforced by geosynthetic. *Comput. Geotech.* **2009**, *36*, 709–717. [\[CrossRef\]](#)
117. Rousseau, J.; Frangin, E.; Marin, P.; Daudeville, L. Multidomain finite and discrete elements method for impact analysis of a concrete structure. *Eng. Struct.* **2009**, *31*, 2735–2743. [\[CrossRef\]](#)
118. Zheng, G.; Jiang, Y.; Han, J.; Liu, Y.-F. Performance of Cement-Fly Ash-Gravel Pile-Supported High-Speed Railway Embankments over Soft Marine Clay. *Mar. Georesour. Geotechnol.* **2011**, *29*, 145–161. [\[CrossRef\]](#)
119. Han, G.-X.; Gong, Q.-M.; Zhou, S.-H. Soil Arching in a Piled Embankment under Dynamic Load. *Int. J. Géoméch.* **2015**, *15*, 04014094. [\[CrossRef\]](#)
120. Briançon, L.; Simon, B. Pile-supported embankment over soft soil for a high-speed line. *Geosynth. Int.* **2017**, *24*, 1–13. [\[CrossRef\]](#)
121. Wheeler, L.N.; Hendry, M.T.; Take, W.A.; Hoult, N.A. Field performance of a peat railway subgrade reinforced with helical screw piles. *Can. Geotech. J.* **2018**, *55*, 1888–1899. [\[CrossRef\]](#)
122. Wang, H.-L.; Chen, R.-P.; Cheng, W.; Qi, S.; Cui, Y.-J. Full-scale model study on variations of soil stress in geosynthetic-reinforced pile-supported track bed with water level change and cyclic loading. *Can. Geotech. J.* **2019**, *56*, 60–68. [\[CrossRef\]](#)
123. Jiang, G.; Chen, W.; Liu, X.; Yuan, S.; Wu, L.; Zhang, C. Field study on swelling-shrinkage response of an expansive soil foundation under high-speed railway embankment loads. *Soils Found.* **2018**, *58*, 1538–1552. [\[CrossRef\]](#)
124. Rowe, R.K.; Li, A.L. Geosynthetic-reinforced embankments over soft foundations. *Geosynth. Int.* **2005**, *12*, 50–85. [\[CrossRef\]](#)
125. Bouassida, M.; Hazzar, L. Comparison between Stone Columns and Vertical Geodrains with Preloading Embankment Techniques. In Proceedings of the 6th International Conference on Case Histories in Geotechnical Engineering, Arlington, VA, USA, 11–16 August 2008; Paper No. 7.18a. pp. 1–12.